

ZeBox: A novel non-intrusive continuous-use technology to trap and kill airborne microbes

Kruttika S. Phadke^{1,2}, Deepak G. Madival^{1,3}, Janani Venkataraman¹, Debosmita Kundu¹, K. S. Ramanujan¹, Nisha Holla¹, Jaywant Arakeri³, Gaurav Tomar³, Santanu Datta^{1,4}, and Arindam Ghatak *¹

¹*Biomoneta Research Private Limited, Bangalore, India 560065*

²*Department of Veterinary Microbiology and Preventive Medicine, Iowa State University, Ames, IA, 50011, USA*

³*Mechanical engineering department, Indian Institute of Science, Bangalore, India 560012*

⁴*Bugworks Research, Bangalore, India 560066*

April 16, 2021

Abstract = 150 words (limit = 150)

Introduction(517)+ Results(2141)+Discussion (394) = 3052 words (limit = 3000)

Figures(6)+Tables(2) = 8 (limit = 7)

References = 53 (limit = 50)

1 Abstract

2 Preventing nosocomial infection is a major unmet need of our times. Existing
3 air decontamination technologies suffer from demerits such as toxicity of
4 exposure, species specificity, noxious gas emission, environment-dependent
5 performance and high power consumption. Here, we present a novel
6 technology called "ZeBox" that transcends the conventional limitations and
7 achieves high microbicidal efficiency. In ZeBox, a non-ionizing electric field
8 extracts naturally charged microbes from flowing air and deposits them on
9 engineered microbicidal surfaces. The surface's three dimensional topography
10 traps the microbes long enough for them to be inactivated. The electric field
11 and chemical surfaces synergistically achieve rapid inactivation of a broad
12 spectrum of microbes. ZeBox achieved near complete kill of airborne microbes
13 in challenge tests (5-9 log reduction) and >90% efficiency in a fully functional
14 stem cell research facility in the presence of humans. Thus, ZeBox fulfills the
15 dire need for a real-time, continuous, safe, trap-and-kill air decontamination
16 technology.

*Corresponding author: arindam@biomoneta.com

17 1 Introduction

18 Microbial load (bacteria, viruses, spores and fungi) in our living, working and
19 hospital space must be reduced to mitigate the transmission of airborne
20 infections. As per CDC (Center for Disease Control, USA)'s recommendation
21 (<https://www.cdc.gov/niosh/topics/hierarchy/default.html>), eliminating
22 microbes at the source as and when produced is the first line of defense against
23 spread of infections. Filtration, electrostatic precipitation, bactericidal gas
24 spraying, ultra-violet germicidal irradiation (UVGI, employing ~ 254 nm
25 radiation), plasma discharge and photo-catalytic oxidation (PCO) are the
26 currently available air decontamination technologies [1]. While some are
27 microbicidal, others only trap microbes. Filtration [2] and electrostatic
28 precipitation [3] belong to the latter category. Microbes trapped inside filters
29 can multiply in situ [4, 5, 6, 7, 8]; such filters are detrimental to indoor air
30 quality and hazardous during their disposal. They also offer high flow
31 resistance which translates to high operating power consumption [9, 10].
32 Electrostatic precipitation uses electric field to attract and trap aerosols
33 pre-charged by corona discharge, but which produces noxious gases like ozone
34 [3, 11]. Its microbicidal action is dubious; in fact electrostatic bioaerosol
35 samplers capture microbes that remain viable [12, 13, 14]. However, because of
36 its low flow resistance, it consumes less power per unit of clean air delivered
37 compared to filtration [3]. Filters made of anti-bacterial fibers have also been
38 developed [15, 16, 17, 18, 19, 20] but their performance remains to be proven
39 under realistic indoor conditions.

40 Bactericidal gas spraying, UVGI, plasma discharge and PCO are
41 microbicidal technologies. Although bactericidal gases and UVGI can sterilize
42 an entire room, they cannot be deployed in human presence. UVGI is used to
43 sterilize upper room air and air circulating through ventilation ducts.
44 However, microbicidal action of UVGI depends on environmental parameters
45 such as humidity [21, 22, 23], is species-specific [24] and requires a minimum
46 duration of exposure to microbes [25]. Exposure of humans to UVGI (due to
47 faulty design, deployment or use of UVGI devices) can damage their eyes and
48 skin [26, 27, 28, 29]. UVGI is used to kill microbes trapped on a filter's surface
49 [30, 31] but then it cannot reach microbes residing beneath the surface.
50 Plasma discharge [32] and PCO [34, 35] both generate ions and/or reactive
51 species, respectively using gas discharge and reaction with an irradiated
52 catalyst. However, they also generate NO_x and ozone [1] and additional
53 methods are necessary to mitigate them [33]. In PCO, convection of gas to the
54 catalyst and the subsequent adsorption, reaction and release of reactive species
55 into the bulk flow is the bottleneck process [36], which results in low clean air
56 delivery rates [1].

57 Given the importance of eliminating airborne infection, a technology
58 that is safe, suitable for continuous use and efficient against a wide variety of
59 airborne microbes is desirable. Here, we describe such a novel technology called
60 "ZeBox"; the name derives from the **Z**eta-potential possessed by microbes,
61 which property is pivotal in trapping them inside the **B**ox-shaped device. In
62 the following, we discuss the working mechanism of ZeBox and demonstrate its
63 efficacy in chamber tests and field studies against a variety of microbes.

64 2 Results

65 **Electrode plates with engineered chemical surfaces form the kill**
66 **cassette.** A row of flat plate electrodes ($10.9\text{ cm} \times 30\text{ cm}$) with alternating
67 polarity are assembled inside a cuboid shaped box with open ends for
68 transmitting flow. A three dimensional hydrocellular microbicidal composite
69 material (US patent no. US 9566363B2, licensed) is layered on to the
70 electrodes. A non-ionizing 3 kV/cm electric field is set up between electrodes
71 by applying direct-current voltage between them. Microbes are trapped and
72 killed inside this “kill cassette”. Axial fans pull microbe laden ambient air
73 through the kill cassette and between the electrode-plates, as shown
74 schematically in figure 1.

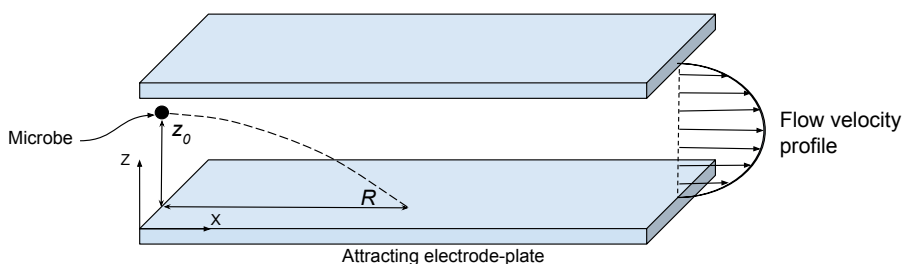


Figure 1: **Microbe in a flow subject to transverse electric field.** A charged microbe deviates from the flow direction due to the electric field between electrode-plates.

75 **Electric field extracts charged microbes from the flow.** Microbes are
76 naturally charged [38, 39]; therefore, in an electric field, they are impelled
77 towards the electrode of opposite polarity. Figure 1 depicts this process
78 schematically. Here, X -axis points along the flow and Z -axis points away from
79 the attracting electrode. A microbe initially at distance z_0 from the attracting
80 electrode travels a distance R in the streamwise direction, called its “range”, as
81 it descends to $z = 0$. Whether or not the microbe hits the electrode depends
82 on its length, the microbe’s initial distance z_0 , strength of the electric field,
83 charge on the microbe and the type of flow (laminar or turbulent). The
84 Reynolds number for the flow between electrodes in ZeBox is $\sim 10^3$ and a
85 rectangular duct flow (or even plane Poiseuille flow) undergoes transition at
86 this Reynolds number and could be turbulent [40, 41]. Analyzing microbe’s
87 motion in a turbulent flow is difficult because of its complicated, stochastic
88 nature; supplementary information S1 analyzes microbe’s motion and its
89 maximum range in a laminar flow instead.

90 Earlier studies on resuspension of dust from flat surfaces due to a flow
91 show that, whenever the hydrodynamic force and torque exerted by the flow
92 exceed those that keep the particles attached to the surface (for example, Van
93 der Waals force), the particles can either detach by lifting off or slide and roll
94 on the surface [42, 43]. In our case, lifting off of microbes from the electrode is
95 unlikely due to the strong electric field, but they can nevertheless slide and roll
96 and thus escape away due to the electrode’s finite length (refer figure 2). Since
97 the microbicidal surface requires a minimum duration of contact to inactivate

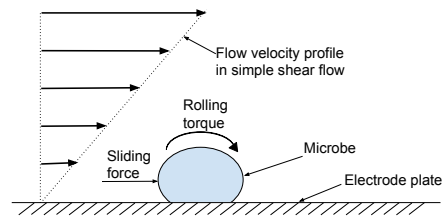


Figure 2: **Microbe sliding and rolling on a flat surface.** Microbes can slide and roll over a flat surface due to hydrodynamic force and torque exerted by the flow.

98 microbes depending on how sensitive or hardy it is, a fraction of the deposited
99 microbes could escape while still viable. Therefore, the ability of the
100 microbicidal surface to trap and hold microbes until they are inactivated
101 becomes important.

102 **Three dimensional topography of the microbicidal surface traps the**
103 **microbe.** The microbicidal surface employed in ZeBox has a highly uneven
104 topography at the microbial scale, populated with well-like depressions to trap
105 and hold microbes. Figures 3a and 3b show the scanning electron microscope
106 (SEM) images of the surface at different magnifications appropriate to the
107 microbial scale. Figure 3c shows streamlines in a numerically simulated two
108 dimensional flow (using OpenFOAM-7) over a surface with square shaped
109 wells, to qualitatively illustrate the kind of flow obtained over an uneven
110 topography. A simple shear flow was imposed on the flow domain (refer figure
111 3c) by moving its uppermost boundary horizontally at constant speed. The
112 flow Reynolds number based on the imposed shear rate and the dimension of
113 the square-shaped well is $\sim 10^{-5}$, which is appropriate to the flow in the
114 neighborhood of the microbicidal surface in ZeBox. The important feature of
115 the flow for our purpose is the recirculating region set up within the wells, in
116 which the streamlines of the flow form closed loops. This feature is quite
117 general for a flow over an uneven topography and which presumably enhances
118 the efficacy of the microbicidal surface further in regard to trapping microbes.
119 Once the microbe falls into one of the wells, brought there either in the course
120 of its rolling over the surface or directly by the electric field, the recirculating
121 flow can confine it to the well for a sufficiently long duration.

122 Table 1 shows the efficacy of microbicidal surfaces (in terms of \log_{10}
123 reduction, where $n\text{-}\log_{10}$ reduction implies reduction in the initial microbial
124 load by a factor of 10^n) with different topographies, which we call 2-D and 3-D
125 surfaces, in flow experiments. A 2-D surface is a single layer of cotton fabric
126 while a 3-D surface is a multilayered 90:10 polyethylene : cotton fabric. In the
127 presence of electric field, 3-D microbicidal surface performs better than the
128 2-D surface. When the electric field is absent, the microbes are not extracted
129 from the flow and hence both surfaces perform similarly.

130 **Electric field and chemical microbicidal-surfaces synergistically**
131 **achieve rapid inactivation of microbes.** In contrast to electrostatic
132 precipitators, the applied electric field in ZeBox plays two roles: it pulls

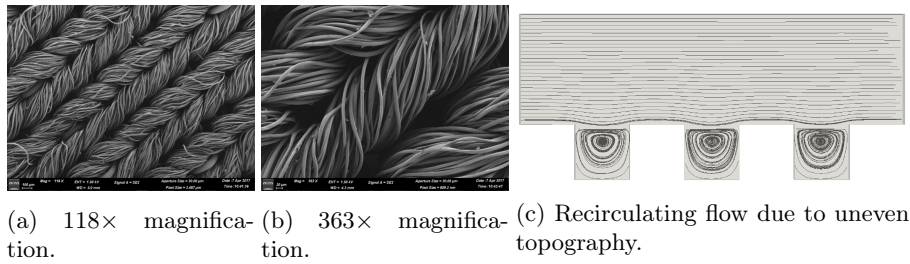


Figure 3: **Topography of the microbicidal surface at microbial scale.** SEM photographs revealing the highly uneven topography of microbicidal surface and the expected flow patterns over it.

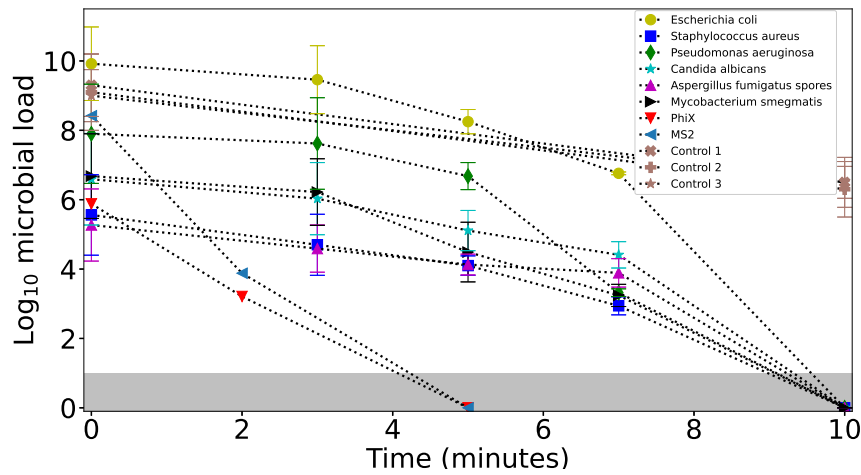
	Microbial load reduction (\log_{10} scale)	
	3-D surface	2-D surface
Without electric field	2.82 ± 0.74	2.13 ± 0.2
With electric field	9.42 ± 1.02	4.68 ± 0.88

Table 1: **Effect of surface topography on microbicidal action.** \log_{10} -reduction in viable microbial load (*E. coli*) achieved by ZeBox with 3-D and 2-D microbicidal surfaces in 10 minutes. Applied electric field = 3 kV/cm. Superscripts show standard deviation.

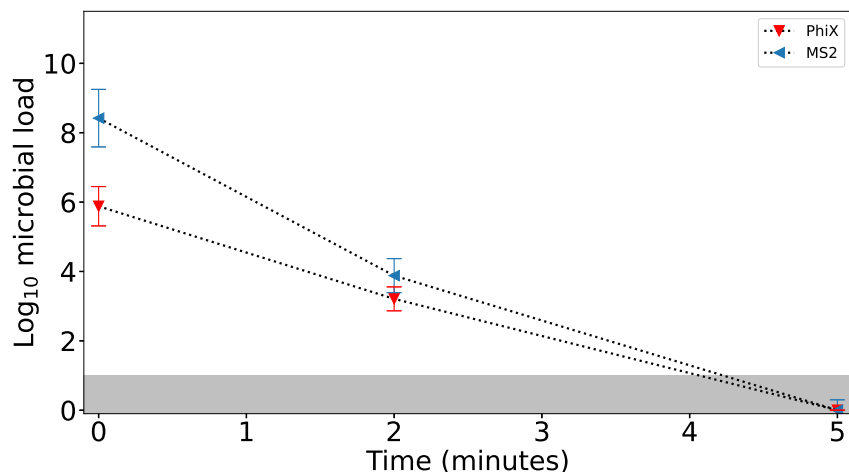
Time (mins)	Microbial load reduction (\log_{10} scale)	
	With electric field	Without electric field
2	3.00 ± 0.39	0.87 ± 0.44
5	5.71 ± 0.19	1.86 ± 0.78
10	8.83 ± 0.69	2.56 ± 1.17

Table 2: **Effect of applied electric field on the efficacy of microbicidal surface.** Effect of 3 kV/cm electric field on the \log_{10} -reduction in viable microbial load (*E. coli*) over the microbicidal surface in spot experiments. Superscripts show standard deviation.

133 microbes from the flow on to the microbicidal surface and then accelerates
 134 their subsequent inactivation. Table 2 shows \log_{10} -reduction in the microbial
 135 load in spot experiments, with 3 kV/cm electric field applied between
 136 electrodes. The microbicidal surface achieves the highest reduction in
 137 microbial load in the presence of the electric field. Quaternary ammonium
 138 compounds (QAC) are membrane-active agents which inactivate microbes by
 139 targeting their cytoplasmic membrane [46, 47, 48, 49], but first, they must
 140 breach the outer cell wall. In the present design, QAC is tethered to the 3-D
 141 surface by long flexible chains, which presumably helps the QAC to orient
 142 itself to puncture holes in the microbe. The external electric field increases the
 143 trans-membrane voltage of the cell above its resting value, leading to an
 144 electric current that presumably flows through these pores as they form the
 145 path of least resistance. This current flow may be analogous to the
 146 electroporation of bacteria in which the pores formed in the cell wall are
 147 stabilized [50]. The intracellular components then leak from the pores, as is



(a) Reduction in microbial load.



(b) Reduction in viral load.

Figure 4: **Reduction of microbial load in test chamber.** Variation of the \log_{10} microbial load over time after ZeBox is turned on in the test chamber. The shaded region indicates limit of detection (LoD). Control 1, 2, 3 refer to control experiments employing respectively microbicidal surface without electric field, control surface with electric field and control surface without electric field.

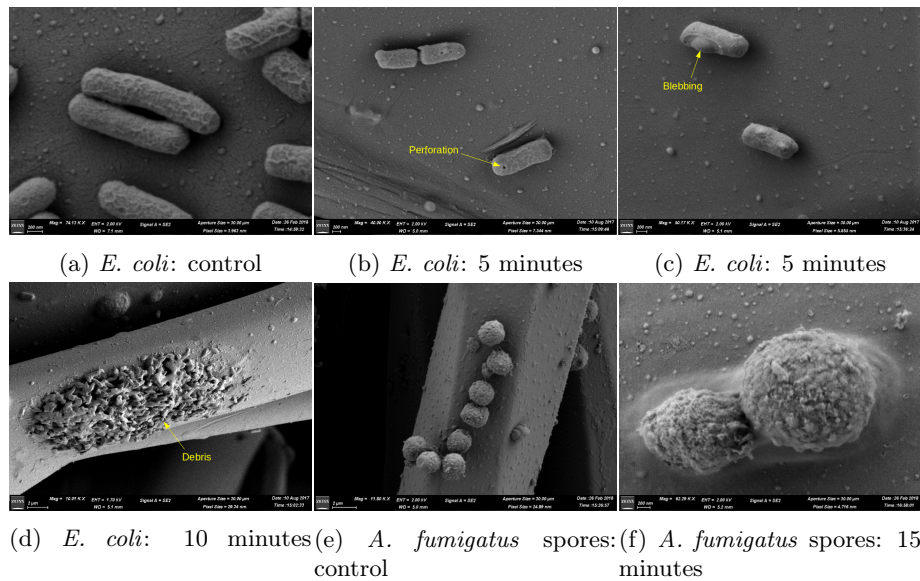


Figure 5: **Microbicidal action of the chemical surface.** SEM images showing microbes on the microbicidal surface being killed by electroporation.

148 seen in the SEM pictures. This process leads to the irreversible killing of the
149 cells. Therefore, the chemical surface in tandem with the electric field displays
150 an enhanced electro-chemical microbicidal action compared to what they
151 would have achieved separately.

152 **ZeBox rapidly reduces microbial load in chamber tests.** The
153 capability of ZeBox to decontaminate a closed space containing airborne
154 microbes was determined by challenge tests [51]. A broad spectrum of
155 microorganisms was employed in the test – standard gram-positive and
156 gram-negative bacteria of ESKAPE group (*Escherichia coli*, *Staphylococcus*
157 *aureus*, *Pseudomonas aeruginosa*), mycobacterium species (*Mycobacterium*
158 *smegmatis*), fungal species (*Aspergillus fumigatus* spores and *Candida*
159 *albicans*) and virus (PhiX 174 coliphage and MS2 coliphage). Among these,
160 MS2 virus is an accepted surrogate for the SARS-CoV2 virus [52, 53]. Figure 4
161 shows the collated data on the variation in \log_{10} microbial load (n - \log_{10}
162 microbial load equals 10^n microbes) over time after ZeBox was turned on.
163 ZeBox proves to be extremely effective in rapidly decreasing the viable
164 microbial load in a closed space. It achieved 9.9 \log_{10} -reduction (i.e.
165 99.999999999% reduction) of *E. coli* in 10 minutes (n \log_{10} -reduction equals
166 reduction by a factor of 10^n). For other microbes ZeBox brought about 5 to 9
167 \log_{10} -reduction (i.e. 99.999-99.9999999% reduction) of the viable microbial
168 load.

169 **SEM images of microbicidal action.** Scanning electron microscopy
170 (SEM) studies were done to see how microbes trapped on the microbicidal
171 surface are killed. *E. coli* and *A. fumigatus* spores were chosen because they
172 form two extremes on the scale of sensitivity, with spores being hardy. Figure

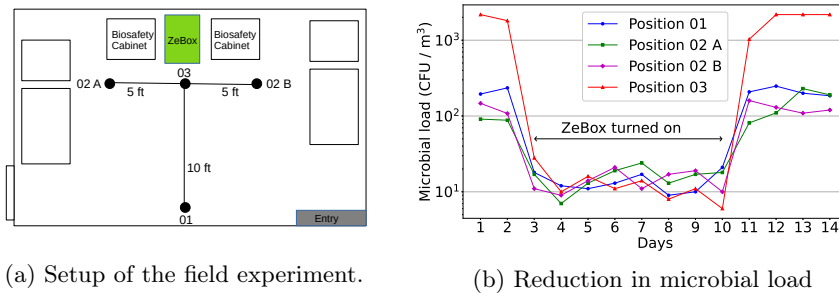


Figure 6: **Field performance of ZeBox.** ZeBox reduces the microbial load in an open room. Measurement locations are indicated by filled circles in the schematic.

173 5a and 5e show the microbes in control conditions. Due to electro-chemical
174 action at the three dimensional microbicidal surface, their cell membrane
175 undergoes morphological changes followed by complete degradation. Figure 5b
176 and 5c, obtained after 5 minutes of contact, reveals puncturing and blebbing
177 of the *E. coli* cell membrane. Ultimately, the cells burst and their intracellular
178 contents spill out (figure 5d and 5f) signaling a complete degradation of the
179 microbes.

180 **ZeBox reduces microbial load in open room.** ZeBox's performance was
181 also tested in a real life setting, i.e. in a room with constant influx of microbes
182 from outside or due to internal sources. A working tissue culture laboratory in
183 a building with central air-conditioning, but without High Efficiency
184 Particulate Air (HEPA) filters, was chosen for the purpose. Figure 6a shows
185 the schematic plan-view of the lab and the measurement locations. The
186 working people in the lab were the primary source of microbial contamination.
187 Figure 6b shows that the microbial load at location-03 where tissue culture
188 work was carried out was >3000 CFU/m³ initially. ZeBox reduced the
189 microbial load in the lab to ~ 10 CFU/m³ within about 3 hours after it was
190 turned on. This low level was consistently maintained so long as ZeBox was
191 operational. When it was turned off at day 10, the microbial load rebounded
192 to its original level. During its operation, ZeBox effectively decontaminated a
193 zone of dimensions ~ 10 feet \times 10 feet (refer figure 6a), which demonstrates its
194 potential to decontaminate a smaller region of interest in a relatively large
195 open room, with continuous movement of personnel and without needing
196 physical partitions.

197 **ZeBox does not produce ozone.** Since ZeBox employs non-ionizing
198 electric field, it does not produce ozone (verified in standardized laboratory
199 tests, data not shown here). This is an immense advantage over conventional
200 microbicidal technologies such as plasma and PCO. Also, it consumes <20
201 Watt-hour of electric energy during its operation.

202 3 Discussion and Conclusions

203 ZeBox technology exploits the fact that microbes (bacteria, viruses, spores and
204 fungi) are naturally charged and therefore can be readily manipulated by an
205 electric field. Using a non-ionizing electric field, microbicidal surfaces with
206 three dimensional topography and electro-chemical kill mechanism, ZeBox
207 achieves significantly higher microbicidal rate compared to other technologies.

208 Knowing the total reduction in microbial load, as shown in figure 4, is
209 inadequate to gauge ZeBox's efficacy because any level of decontamination
210 may be achieved given sufficient time. Therefore, an overall microbicidal
211 efficiency must be determined while factoring in the time of operation as well
212 as the volume of the room being decontaminated. Towards this end, we may
213 think in terms of the number of nominal air changes in a room achieved in a
214 given duration and the consequent reduction in microbial load for each air
215 change. In time t , Qt/V number of nominal air changes is achieved, where Q
216 is the air flow rate through ZeBox and V is the volume of the room. If η is the
217 corresponding microbicidal efficiency, then N_0 initial number of viable
218 microbes in the room decreases to $N = N_0(1 - \eta)^{Qt/V}$ after time t . Using this
219 formula and the latest-time data from figure 4 whose ordinate is $\log_{10} N$, we
220 may back-calculate η for a specified time duration. The microbicidal efficiency
221 of ZeBox lies in the range of 83-99 % for all the tests. Considering the variety
222 of sensitive and hardy microbes employed, ZeBox is about equally effective
223 against all of them. Supplementary information S2 provides a theoretical
224 estimation of the microbicidal efficiency of ZeBox and shows that the efficiency
225 deduced from experimental data is aligned with it.

226 Airborne microbes of size $< 2 \mu\text{m}$ can remain suspended in air for
227 several hours before settling down and therefore must be inactivated to reduce
228 the transmission of infections. ZeBox technology presents a universal solution
229 because:

- 230 • Freely floating microbes are trapped and killed with high efficiency,
231 eliminating the possibility of future growth.
- 232 • The airflow is parallel to antimicrobial surfaces with almost no
233 resistance; therefore, unlike HEPA filters, it has low energy utilization.
- 234 • There are no chemical emissions or production of free radicals or ozone;
235 the technology is safe for continuous use in the presence of humans and
236 animals.
- 237 • It is equally effective for different varieties of sensitive and hardy
238 microbes.

239 Materials and methods

240 Challenge tests

241 **A. Test setup** An air-sealed test chamber of dimensions 3 ft \times 4 ft \times 3 ft
242 (approximately 1000 liters in volume) was built with multiple sampling and
243 nebulization ports. The environmental parameters such as relative humidity
244 and temperature could be monitored using a probe located inside the

245 chamber. During experiments, various microorganisms were aerosolized using
246 a 6-jet collision nebulizer (MESA LABS, BGI) into the chamber, and the
247 device efficiency was monitored by collecting and measuring microbial
248 concentration at different time intervals. A second test chamber of dimensions
249 3ft x 2.5 ft x 1 ft (approximately 220 liters in volume) placed inside a biosafety
250 cabinet, with similar aerosolization and sampling port configuration, was used
251 for tests with viruses.

252 **B. Cultivation of test microorganisms** To validate the efficiency of the
253 decontamination device, *Escherichia coli* (MTCC 40), *Pseudomonas*
254 *aeruginosa* (MTCC 424), *Staphylococcus aureus* (MTCC 96), *Candida albicans*
255 (MTCC 584), *Aspergillus fumigatus* (MTCC 2544), *Mycobacterium smegmatis*
256 (MTCC 6), MS2 coliphage (ATCC 15597-B1) and PhiX 174 coliphage (ATCC
257 13706-B1) were used. For growing *Escherichia coli*, *Pseudomonas aeruginosa*
258 and *Staphylococcus aureus*, Luria broth was used. For growing *Candida*
259 *albicans*, Potato dextrose broth was used, while for *M. smegmatis*,
260 Middlebrook 7H9 broth was used. For enumeration of *E.coli*, samples were
261 plated on Luria Bertani agar; Ceftrimide agar was used as a selective for the
262 growth and isolation of *Pseudomonas aeruginosa*. Ceftrimide inhibits the
263 growth of many microorganisms while allowing *Pseudomonas aeruginosa* to
264 develop typical colonies. For quantification of *Staphylococcus*, Mannitol Salt
265 Agar plates were used. *Candida albicans* and *Aspergillus fumigatus* spores
266 were enumerated using Rose-Bengal Chloramphenicol Agar plates. Coliphages
267 were cultivated using standard method described in ATCC manual. For all
268 microbiological nutrient media were manufactured by HiMedia Laboratories,
269 India unless mentioned otherwise.

270 **C. Aerosolization of test microbes** A 6-jet Collision nebulizer (MESA
271 LABS, BGI) was used to aerosolize the test microbes into the test chamber.
272 Dry air from a compressed air cylinder at a pressure of 10 psi was used to
273 operate the nebulizer. The nebulizer produces bioaerosols of a 2-5 μm diameter
274 that allows them to float in the air present in the test chamber for a definite
275 period. The length of the nebulization period varied depending on the type of
276 experiment and microorganism, but typically ranged between 30-40 minutes.

277 **D. Sampling of air for viable microbes** The airborne survival of the test
278 microbe and the activity of the air decontamination devices were determined
279 by collecting the air from the chamber at the rate of 12.5 liter/min using SKC
280 biosampler [54], filled with sterile buffer (1x Phosphate buffer saline, pH 7.2).
281 Collected samples were analyzed to understand the quantity of viable
282 microorganism present by diluting and plating them onto suitable growth
283 media. The plated samples were incubated at 37 ± 2 $^{\circ}\text{C}$ for bacteria and 25 ± 2
284 $^{\circ}\text{C}$ for fungal species and allowed to grow for 18-48 hours as mentioned in the
285 ATCC/MTCC manual, individual colonies were enumerated, and the final
286 concentration of the microbial load was calculated thereafter. For enumerating
287 coliphages collected from the chamber, Double agar overlay method was used
288 for subsequent plaque assay [55]. *E. coli* ATCC 15597 and *E. coli* ATCC
289 13706 were used as a host in plaque assays for MS2 and PhiX174, respectively.
290 Plaques were counted after 24 hour incubation at 37 ± 2 $^{\circ}\text{C}$.

291 **E. Spot experiments** *E. coli* cells were grown in the standard medium. A
292 known titre of cells were spotted onto a 25 mm² surface and incubated for
293 various time duration, both with and without electric field. Surfaces were
294 resuspended in 500 μ l of sterile 1X PBS, which was then plated on standard
295 agar plates to enumerate the microbes.

296 **F. Limit of Detection** Microbial enumeration is guided by two parameters,
297 Limit of Detection (LOD) and Limit of Quantification (LOQ). For the present
298 assays used to quantify the microbial load inside the test chamber, the LOD
299 was 10 CFU for bacterial and fungal load and 5 PFU for viral load. However,
300 LOD is always less than LOQ [56]. In many of our experimental analysis, post
301 operating ZeBox device, the microbial detected numbers were in around LOD
302 and hence, the exact LOQ was often indeterminant.

303 **G. SEM analysis of trapped microbes to decipher the mechanism of**
304 **kill** 3D surfaces were stripped off from the electrode plates post operating
305 the device against *E.coli* under challenge test under various time course, and
306 treated with 2.5% glutaraldehyde in 0.1 M phosphate buffer (pH 7.2) for 24 hrs
307 at 4 °C. The samples were dehydrated in series of graded ethanol solutions and
308 subjected to critical point drying with CPD unit. The analyzed samples were
309 mounted over the stud with double-sided carbon conductivity tape, and a thin
310 layer of gold coat over the samples was done by using an automated sputter
311 coater (EMITECK K550X Sputter Coater from EM Scientific Services) for 3
312 minutes and analyzed under Field Emission Scanning Electron Microscope
313 (MERLIN Compact VP from M/s.Carl Ziess). The set parameters were:
314 Working Distance= 5-6 mm, EHT range= 2-4 kV, Range of Magnification= 70
315 KX, detectors=SE2 And InLens, machine under high vacuum.

316 **Field tests**

317 **H. Air sample collection** A working tissue culture laboratory in a
318 national stem cell research facility was chosen for study. This laboratory was
319 situated in a building which had central airconditioning but the absence of a
320 HEPA-enabled air handling unit resulted in frequent contamination of tissue
321 culture samples. A handheld air sampler (SAS Super 100) was used, which
322 could sample 100 liters of air per minute. Tryptic Soy Agar and Sabouraud
323 dextrose agar plates were used to sample bacteria and fungi, respectively from
324 the air. A fixed volume of air was sampled using the bio-sampler. Plates were
325 placed in and removed from the bio-sampler in an aseptic manner. Plates were
326 incubated at 25 \pm 2 °C (for fungal cultivation) and 37 \pm 2 °C (for bacterial
327 cultivation) for 48 hours. Post-incubation, the number of colonies appeared
328 were enumerated and converted to CFU/m³ using statistical conversion
329 provided by the manufacturer. Control plates were used to ensure the sterility
330 of the entire process.

331 **Acknowledgments**

332 The authors acknowledge the Electron Microscopy Facility at Bangalore Life
333 Science Cluster (C-CAMP, NCBS, inStem) for technical assistance in Scanning

334 Electron microscopy imaging. Financial assistance was received from
335 Department of Biotechnology- Biotechnology Industry Research Assistance
336 Council (DBT-BIRAC), Govt. of India under Small Business Innovation
337 Research Initiative (SBIRI) (Grant no. BT/SBIRI1372/31/16), COVID-19
338 Consortium (Grant no. BT/COVID0025/01/20), and from Karnataka
339 Innovation and Technology Society (KITS) Department of Electronics, IT, Bt
340 and S&T, Government of Karnataka, under Ideas2PoC Grant.

341 Author contributions

342 KSP, DK carried out experiments designed and supervised by SD, AG. DM,
343 NH carried out theoretical and numerical work supervised by JA, GT. JV,
344 KSR, SD, AG conceptualized and designed the technology. JV, AG secured
345 and managed funding.

346 Competing interests

347 JA, GT declare no competing interests. SD is Director on Biomoneta board.
348 The rest of the authors are, or were, employees of Biomoneta Research Private
349 Limited, Bangalore, India 560065.

350 References

- 351 [1] Zhang Y, Mo J, Li Y, Sundell J, Wargocki P, Zhang J, Little JC, Corsi R,
352 Deng Q, Leung MH, Fang L. Can commonly-used fan-driven air cleaning
353 technologies improve indoor air quality? A literature review. *Atmospheric*
354 *Environment*. 2011 Aug;45(26):4329-43.
- 355 [2] Liu G, Xiao M, Zhang X, Gal C, Chen X, Liu L, Pan S, Wu J, Tang L,
356 Clements-Croome D. A review of air filtration technologies for sustainable
357 and healthy building ventilation. *Sustainable cities and society* 2017
358 Jul;32:375–396.
- 359 [3] Afshari A, Ekberg L, Forejt L, Mo J, Rahimi S, Siegel J, Chen W,
360 Wargocki P, Zurami S, Zhang J. Electrostatic Precipitators as an Indoor
361 Air Cleaner—A Literature Review. *Sustainability*. 2020 Jan;12(21):8774.
- 362 [4] Simmons RB, Crow SA. Fungal colonization of air filters for use in
363 heating, ventilating, and air conditioning (HVAC) systems. *Journal of*
364 *industrial microbiology*. 1995 Jan;14(1):41-5.
- 365 [5] Kemp SJ, Kuehn TH, Pui DY, Vesley D, Streifel AJ. Filter collection
366 efficiency and growth of microorganisms on filters loaded with outdoor
367 air. *ASHRAE Transactions*. 1995 Jan:228-38.
- 368 [6] Maus R, Goppelsröder A, Umhauer H. Survival of bacterial and mold
369 spores in air filter media. *Atmospheric Environment*. 2001
370 Jan;35(1):105-13.

- 371 [7] Forthomme A, Joubert A, Andrès Y, Simon X, Duquenne P, Bemer D, Le
372 Coq L. Microbial aerosol filtration: Growth and release of a
373 bacteria–fungi consortium collected by fibrous filters in different operating
374 conditions. *Journal of aerosol science*. 2014 Jun;72:32-46.
- 375 [8] Morisseau K, Joubert A, Le Coq L, Andres Y. Quantification of the
376 fungal fraction released from various preloaded fibrous filters during a
377 simulated ventilation restart. *Indoor air*. 2017 May;27(3):529-38.
- 378 [9] Stephens B, Novoselac A, Siegel JA. The effects of filtration on pressure
379 drop and energy consumption in residential HVAC systems (RP-1299).
380 *HVAC&R Research*. 2010 May;16(3):273-94.
- 381 [10] Xu T, Lan CH, Jeng MS. Performance of large fan-filter units for
382 cleanroom applications. *Building and Environment*. 2007
383 Jun;42(6):2299-304.
- 384 [11] Boelter KJ, Davidson JH. Ozone generation by indoor, electrostatic air
385 cleaners. *Aerosol science and technology*. 1997 Jan 1;27(6):689-708.
- 386 [12] Gerone PJ, Couch RB, Keefer GV, Douglas RG, Derrenbacher EB,
387 Knight V. Assessment of experimental and natural viral aerosols.
388 *Bacteriological reviews*. 1966 Sep;30(3):576.
- 389 [13] Mainelis G. Collection of airborne microorganisms by electrostatic
390 precipitation. *Aerosol Science and Technology*. 1999 Feb;30(2):127-44.
- 391 [14] Ghosh B, Lal H, Srivastava A. Review of bioaerosols in indoor
392 environment with special reference to sampling, analysis and control
393 mechanisms. *Environment international*. 2015 Dec;85:254-72.
- 394 [15] Zhang L, Luo J, Menkhaus TJ, Varadaraju H, Sun Y, Fong H.
395 Antimicrobial nano-fibrous membranes developed from electrospun
396 polyacrylonitrile nanofibers. *Journal of membrane science*. 2011
397 Mar;369(1-2):499-505.
- 398 [16] Mei Y, Yao C, Fan K, Li X. Surface modification of polyacrylonitrile
399 nanofibrous membranes with superior antibacterial and easy-cleaning
400 properties through hydrophilic flexible spacers. *Journal of membrane
401 science*. 2012 Nov;417:20-7.
- 402 [17] Zhong Z, Xu Z, Sheng T, Yao J, Xing W, Wang Y. Unusual air filters
403 with ultrahigh efficiency and antibacterial functionality enabled by ZnO
404 nanorods. *ACS applied materials & interfaces*. 2015 Sep;7(38):21538-44.
- 405 [18] Liu S, Zhao J, Ruan H, Wang W, Wu T, Cui W, Fan C. Antibacterial
406 and anti-adhesion effects of the silver nanoparticles-loaded poly
407 (L-lactide) fibrous membrane. *Materials Science and Engineering: C*. 2013
408 Apr;33(3):1176-82.
- 409 [19] Mei Y, Yao C, Li X. A simple approach to constructing antibacterial and
410 anti-biofouling nanofibrous membranes. *Biofouling*. 2014
411 Mar;30(3):313-22.

- 412 [20] Jeong SB, Heo KJ, Lee BU. Antimicrobial Air Filters Using Natural Sea
413 Salt Particles for Deactivating Airborne Bacterial Particles. *International*
414 *journal of environmental research and public health*. 2020 Jan;17(1):190.
- 415 [21] Xu P, Kujundzic E, Peccia J, Schafer MP, Moss G, Hernandez M, Miller
416 SL. Impact of environmental factors on efficacy of upper-room air
417 ultraviolet germicidal irradiation for inactivating airborne mycobacteria.
418 *Environmental science & technology*. 2005 Dec;39(24):9656-64.
- 419 [22] Ko G, First MW, Burge HA. Influence of relative humidity on particle
420 size and UV sensitivity of *Serratia marcescens* and *Mycobacterium bovis*
421 BCG aerosols. *Tubercle and Lung Disease*. 2000 Aug;80(4-5):217-28.
- 422 [23] Tang JW. The effect of environmental parameters on the survival of
423 airborne infectious agents. *Journal of the Royal Society Interface*. 2009
424 Dec 6;6(suppl-6):S737-46.
- 425 [24] Memarzadeh F, Olmsted RN, Bartley JM. Applications of ultraviolet
426 germicidal irradiation disinfection in health care facilities: effective
427 adjunct, but not stand-alone technology. *American journal of infection*
428 *control*. 2010 Jun;38(5):S13-24.
- 429 [25] Mamahlodi MT. Potential benefits and harms of the use of UV radiation
430 in transmission of tuberculosis in South African health facilities. *Journal*
431 *of public health in Africa*. 2019 May;10(1).
- 432 [26] Nardell EA, Bucher SJ, Brickner PW, Wang C, Vincent RL,
433 Becan-McBride K, James MA, Michael M, Wright JD. Safety of
434 upper-room ultraviolet germicidal air disinfection for room occupants:
435 results from the Tuberculosis Ultraviolet Shelter Study. *Public health*
436 *reports*. 2008 Jan;123(1):52-60.
- 437 [27] Zaffina S, Camisa V, Lembo M, Vinci MR, Tucci MG, Borra M,
438 Napolitano A, Cannatà V. Accidental exposure to UV radiation produced
439 by germicidal lamp: case report and risk assessment. *Photochemistry and*
440 *photobiology*. 2012 Jul;88(4):1001-4.
- 441 [28] Vaidya MU, Gangakhedkar GR, Shetty AN, Waghalkar PV. A rare
442 occurrence of accidental exposure to UV radiation among operating
443 theatre personnel. *Indian journal of anaesthesia*. 2020 Mar;64(3):230.
- 444 [29] Brickner PW, Vincent RL. Ultraviolet Germicidal Irradiation Safety
445 Concerns: A Lesson from the Tuberculosis Ultraviolet Shelter Study
446 Murphy's Law Affirmed. *Photochemistry and photobiology*. 2013
447 Jul;89(4):819-21.
- 448 [30] Kujundzic E, Matalakah F, Howard CJ, Hernandez M, Miller SL. UV air
449 cleaners and upper-room air ultraviolet germicidal irradiation for
450 controlling airborne bacteria and fungal spores. *Journal of Occupational*
451 *and Environmental Hygiene*. 2006 Oct;3(10):536-46.
- 452 [31] Nakpan W, Yermakov M, Indugula R, Reponen T, Grinshpun SA.
453 Inactivation of bacterial and fungal spores by UV irradiation and gaseous
454 iodine treatment applied to air handling filters. *Science of The Total*
455 *Environment*. 2019 Jun;671:59-65.

- 456 [32] Bahri M, Haghghat F. Plasma-B ased Indoor Air Cleaning Technologies:
457 The State of the Art Review. CLEAN–Soil, Air, Water. 2014
458 Dec;42(12):1667-80.
- 459 [33] Tang X, Feng F, Ye L, Zhang X, Huang Y, Liu Z, Yan K. Removal of
460 dilute VOCs in air by post-plasma catalysis over Ag-based composite
461 oxide catalyts. Catalysis today. 2013 Aug;211:39-43.
- 462 [34] Mamaghani AH, Haghghat F, Lee CS. Photocatalytic oxidation
463 technology for indoor environment air purification: the state-of-the-art.
464 Applied Catalysis B: Environmental. 2017 Apr;203:247-69.
- 465 [35] Chen F, Yang X, Mak HK, Chan DW. Photocatalytic oxidation for
466 antimicrobial control in built environment: a brief literature overview.
467 Building and environment. 2010 Aug;45(8):1747-54.
- 468 [36] Zhong L, Haghghat F. Photocatalytic air cleaners and materials
469 technologies–abilities and limitations. Building and Environment. 2015
470 Sep;91:191-203.
- 471 [37] Mo J, Zhang Y, Xu Q, Zhu Y, Lamson JJ, Zhao R. Determination and
472 risk assessment of by-products resulting from photocatalytic oxidation of
473 toluene. Applied Catalysis B: Environmental. 2009 Jul;89(3-4):570-6.
- 474 [38] Wei K, Zou Z, Yao M. Charge levels and Gram (\pm) fractions of
475 environmental bacterial aerosols. Journal of aerosol science. 2014
476 Aug;74:52-62.
- 477 [39] Shen F, Kai W, Yao M. Negatively and positively charged bacterial
478 aerosol concentration and diversity in natural environments. Chinese
479 Science Bulletin. 2013 Sep;58(26):3169-76.
- 480 [40] Tosun I, Uner D, Ozgen C. Critical Reynolds number for Newtonian flow
481 in rectangular ducts. Industrial & engineering chemistry research. 1988
482 Oct;27(10):1955-7.
- 483 [41] Kundu P.K., Cohen I.M., Hu H.H. Fluid Mechanics. Academic press,
484 London (pp. 516); 2008.
- 485 [42] Kassab AS, Ugaz VM, King MD, Hassan YA. High resolution study of
486 micrometer particle detachment on different surfaces. Aerosol Science and
487 Technology. 2013 Apr;47(4):351-60.
- 488 [43] Soltani M, Ahmadi G. On particle adhesion and removal mechanisms in
489 turbulent flows. Journal of Adhesion Science and Technology. 1994
490 Jan;8(7):763-85.
- 491 [44] Mainelis G, Willeke K, Baron P, Reponen T, Grinshpun SA, Górný RL,
492 Trakumas S. Electrical charges on airborne microorganisms. Journal of
493 Aerosol Science. 2001 Sep;32(9):1087-110.
- 494 [45] Lee SA, Willeke K, Mainelis G, Adhikari A, Wang H, Reponen T,
495 Grinshpun SA. Assessment of electrical charge on airborne
496 microorganisms by a new bioaerosol sampling method. Journal of
497 occupational and environmental hygiene. 2004 Mar;1(3):127-38.

- 498 [46] Hugo WB. The mode of action of antibacterial agents. *Journal of Applied*
499 *Bacteriology*. 1967 Apr;30(1):17-50.
- 500 [47] Denyer SP. Mechanisms of action of antibacterial biocides. *International*
501 *biodeterioration & biodegradation*. 1995 Oct;36(3-4):227-45.
- 502 [48] McDonnell G, Russell AD. Antiseptics and disinfectants: activity, action,
503 and resistance. *Clinical microbiology reviews*. 1999 Jan;12(1):147-79.
- 504 [49] Tischer M, Pradel G, Ohlsen K, Holzgrabe U. Quaternary ammonium
505 salts and their antimicrobial potential: targets or nonspecific
506 interactions?. *ChemMedChem*. 2012 Jan;7(1):22-31.
- 507 [50] Kotnik T, Rems L, Tarek M, Miklavčič D. Membrane electroporation and
508 electropermeabilization: mechanisms and models. *Annual review of*
509 *biophysics*. 2019 May;48:63-91.
- 510 [51] Jose S, Phadke KS, Venkatraman J, Krishna B, Sampath S, Datta S,
511 Nagaraj S, Ghatak A. Trap and kill of environmental microbes:
512 Validation of a novel decontamination technology in Hospital ICU setting.
513 *medRxiv*. 2020 Jan.
- 514 [52] Li DT, Samaranayake LP, Leung YY, Neelakantan P. Facial protection in
515 the era of COVID-19: A narrative review. *Oral diseases*. 2020 Jun 7.
- 516 [53] Coulliette AD, Perry KA, Fisher EM, Edwards JR, Shaffer RE,
517 Noble-Wang J. MS2 coliphage as a surrogate for 2009 pandemic influenza
518 A (H1N1) virus (pH1N1) in surface survival studies on N95 filtering
519 facepiece respirators. *Journal of the International Society for Respiratory*
520 *Protection*. 2014 Jan;21(1):14.
- 521 [54] Li J, Leavey A, Wang Y, O'Neil C, Wallace MA, Burnham CA, Boon AC,
522 Babcock H, Biswas P. Comparing the performance of 3 bioaerosol
523 samplers for influenza virus. *Journal of aerosol science*. 2018
524 Jan;115:133-45.
- 525 [55] Kropinski AM, Mazzocco A, Waddell TE, Lingohr E, Johnson RP.
526 Enumeration of bacteriophages by double agar overlay plaque assay.
527 *In: Bacteriophages 2009* (pp. 69-76). Humana Press.
- 528 [56] Armbruster DA, Pry T. Limit of blank, limit of detection and limit of
529 quantitation. *The clinical biochemist reviews*. 2008 Aug;29(Suppl 1):S49.

530 Supplementary information

531 **S1. Range of microbes.** To analyze microbe's motion in laminar flow
532 between electrode-plates we adopt the following approximations: (1) The flow
533 is identical to that between infinitely wide plates, which is justified because
534 $W/H \gg 1$, where H is the gap between electrode-plates and W is their width
535 (perpendicular to the flow direction); (2) The flow is fully developed, which is
536 justified because $L/H \gg 1$, where L is the length of electrode-plates along the
537 flow direction; (3) The microbes move with the flow except when electric force
538 acts on them, which is justified because the Stokes number of microbes (a
539 measure of its inertial response to changes in the flow) is $\ll 1$; (4) Self weight
540 of microbes is negligible compared to the electric forces acting on them,
541 because of their extremely small size ($< 5 \mu\text{m}$).

542 The orientation of our coordinate system is shown in figure 1. A steady,
543 unidirectional, incompressible, fully-developed flow is governed by [1]:

$$\frac{du}{dx} = 0 \quad (\text{Mass conservation}) \quad (1)$$

$$\frac{dp}{dx} = \mu \frac{d^2u}{dz^2} \quad (\text{Momentum conservation}) \quad (2)$$

544 where u is the flow velocity along X direction, p is pressure and μ is dynamic
545 viscosity of the fluid. Since, subject to our assumptions, u depends only on z ,
546 mass conservation in Eqn. 1 is automatically satisfied. Since the flow is
547 induced by imposing a pressure difference between the ends of the
548 electrode-plates, the pressure gradient dp/dx is a constant. Therefore,
549 momentum conservation in Eqn. 2 is satisfied if u is a quadratic function of z .
550 We assume it to be of the form, $u = Az(H - z)$, because this automatically
551 satisfies the no-slip boundary condition on the electrode-plates located at
552 $z = 0, H$. The constant A is determined by computing the volumetric flow rate
553 and equating it to the known value Q , $W \int_0^H dz u = Q$, which yields:

$$u(z) = \frac{6Q}{WH^3} z(H - z) \quad (3)$$

554 where Q is the volumetric flow rate of air between the electrode-plates. The
555 flow velocity varies only along Z direction, being maximum midway between
556 the plates and zero at the plates themselves (no-slip condition). Because the
557 Reynolds number of microbe's motion is $\ll 1$, due to its small size and small
558 speeds, only Stokes drag force is exerted by the ambient fluid, $F_{\text{drag}} = 6\pi\mu wa$,
559 where μ is the dynamic viscosity of air. We have assumed that the microbe
560 can be approximated by an equivalent sphere of radius a . The drag
561 counterbalances the electric force on the microbe, $F_{\text{electric}} = qE$, where q is the
562 surface charge on the microbe and E is the strength of the applied electric
563 field. Equating the two forces yields for the settling velocity:

$$w = \frac{qE}{6\pi\mu a} \quad (4)$$

564 While drifting towards the electrode-plate the microbe also travels a
565 distance R in the flow direction, which we call its "range", refer figure 1. If z_0

566 is the initial distance of the microbe from the attracting electrode-plate at its
 567 entrance $x = 0$, then the time T needed for the microbe to hit the
 568 electrode-plate is, $T = z_0/w$. After time t , the vertical location of the microbe
 569 initially located at z_0 will be $z = z_0 - wt$. Then, from eqn. 3, the microbe's
 570 streamwise speed at that time will be $u(z_0 - wt)$. The microbe will hit the
 571 electrode-plate in time $T = z_0/w$ (assuming sufficient plate length). Therefore
 572 the range of the microbe beginning at location z_0 is given by
 573 $R(z_0) = \int_0^T dt u(z_0 - wt)$. Changing the integration variable to $z = z_0 - wt$
 574 transforms the integral to: $R(z_0) = w^{-1} \int_0^{z_0} dz u(z)$. Substituting from eqn. 3
 575 and integrating yields:

$$R(z_0) = \frac{6Qz_0^2}{WH^3w} \left(\frac{H}{2} - \frac{z_0}{3} \right), \quad 0 \leq z_0 \leq H \quad (5)$$

576 The microbe that is farthest from the attracting electrode-plate, i.e. at
 577 $z_0 = H$, has the maximum range:

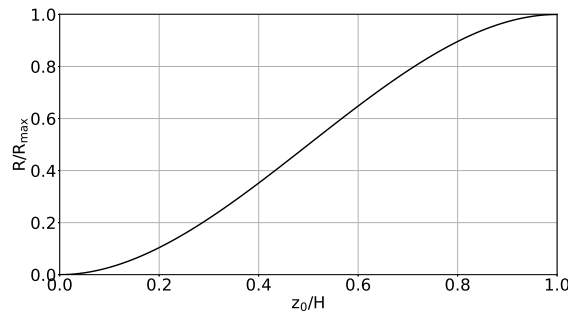
$$R_{\max} = \frac{Q}{Ww} \quad (6)$$

578 All the microbes entering ZeBox will hit the electrode-plate if its length
 579 is not less than the maximum range of the microbes, i.e. if $L \geq R_{\max}$. Eq 5 for
 580 the range is visualized more easily if we divide it through by R_{\max} , Eq 6, and
 581 rewrite it in the following dimensionless form:

$$\frac{R}{R_{\max}} = 6 \left(\frac{z_0}{H} \right)^2 \left(\frac{1}{2} - \frac{(z_0/H)}{3} \right), \quad 0 \leq \frac{z_0}{H} \leq 1 \quad (7)$$

582 Assuming that all the trapped microbes are killed, Eq 7 plotted in
 583 supplementary figure 7 completely determines the microbicidal efficiency of
 584 ZeBox, as per the present model. Here, "microbicidal efficiency" is defined as
 585 the fraction of microbes entering electrode-plates that hit it and are
 586 inactivated, assuming a uniform distribution at the entrance. Using
 587 supplementary figure 7, the microbicidal efficiency is found as follows. We first
 588 compute L/R_{\max} given the operating parameters. If $L/R_{\max} \geq 1$, then the
 589 microbicidal efficiency is of course 100%. Otherwise, we locate its value on the
 590 vertical axis of supplementary figure 7 and using the curve find the
 591 corresponding value on the horizontal axis, which gives the microbicidal
 592 efficiency. Therefore, L/R_{\max} alone determines the microbicidal efficiency of
 593 ZeBox according to the present model.

594 **S2. Microbicidal efficiency of ZeBox.** A microbe in an ionic solution is
 595 surrounded by a diffuse double layer of ions of molecular dimensions. The
 596 Debye length (κ^{-1}), which is a measure of the thickness of the double layer,
 597 lies in the range: $1 < \kappa^{-1} < 10$ nm [2]. Since the microbe's size $a \sim 1$ μ m,
 598 $\kappa a \gg 1$ for microbes. The magnitude of the measured zeta potential (ζ) of
 599 microbes in phosphate-buffer solution lies in the range 1 to 30 mV. Considering
 600 the worst-case-scenario, we may take $\zeta = 1$ mV and $\kappa a = 100$. The number of
 601 elementary charges n on the microbe may then be estimated as [2]:



Supplementary figure 7: **Range of a microbe.** A microbe initially at distance z_0/H from the attracting electrode-plate hits it at a distance R/R_{\max} .

$$n \approx \frac{4\pi\epsilon_r\epsilon_0\zeta a(1 + \kappa a)}{e} \quad (8)$$

602 where ϵ_r is the dielectric constant of the solution, $\epsilon_0 = 8.9 \times 10^{-12}$ F/m is the
603 permittivity of vacuum and $e = 1.6 \times 10^{-19}$ C is the magnitude of the
604 elementary charge. Eqn. 8 is derived from the linearized Poisson-Boltzmann
605 equation governing the variation of electric potential due to distribution of
606 ions in the diffuse layer surrounding a charged sphere; the linearization is a
607 consequence of the Debye-Hückel approximation which is applicable when zeta
608 potential is small (compared to ~ 25 mV at 25 $^{\circ}$ C) [2]. For a measured
609 dielectric constant of 78.5 for the buffer solution, Eqn. 8 reveals $n > 5000$
610 elementary charges. Even allowing for an order-of-magnitude error and
611 assuming $n > 500$ instead, Eqn. 4 yields a settling velocity of $w > 7$ cm/s, for
612 $E = 3$ kV/cm in air.

613 Since the flow rate between a pair of electrode-plates is $Q < 3$ cfm and
614 the electrode-plate width $W = 10.9$ cm, Eqn. 6 shows that $R_{\max} < 19$ cm. In
615 comparison, ZeBox employs 30 cm long electrode-plates. Although in theory it
616 implies 100 % microbicidal efficiency for ZeBox, the present model is only
617 approximate because it does not account for the effects of possible turbulence
618 in the flow and slippage of microbes on the surface. In reality, as mentioned in
619 the Results section, we obtain 83-99 % microbicidal efficiency for ZeBox as
620 deduced from the measured microbial load reduction.

621 References

- 622 [1] Kundu P.K., Cohen I.M., Hu H.H. Fluid Mechanics. Academic press,
623 London (pp. 516); 2008.
- 624 [2] Hiemenz P. C., Rajagopalan R. Principles of Colloid and Surface
625 Chemistry.